Wall fluidization in two acts: from stiff to soft roughness
Electronic Supplementary Information (ESI)

Ladislav Derzsi,[1,*] Daniele Filippi,[1] Matteo Lulli,[2] Giampaolo Mistura,[1] Massimo Bernaschi,[3] Piotr Garstecki,[4] Mauro Sbragaglia,[2,†] and Matteo Pierno[1,‡]

[1] *Dipartimento di Fisica e Astronomia "G. Galilei" - DFA, Università di Padova, Via F. Marzolo 8, 35131 Padova (PD), Italy*

[2] *Dipartimento di Fisica, Università di Roma 2 "Tor Vergata", Via della Ricerca Scientifica 1, 00133 Roma (RM), Italy*

[3] *Istituto per le Applicazioni del Calcolo CNR, Via dei Taurini 19, 00185 Rome, Italy*

[4] *Institute of Physical Chemistry of the Polish Academy of Sciences, Kasprzaka 44/52, 01-224 Warsaw, Poland*

I. EXPERIMENTAL DETAILS

A. Roughness Parameter

The experimental details including fabrication of microfluidics channels, walls texturing, emulsion preparation, flow visualization setup and algorithms for Particle Tracking Velocimetry are described in [1]. In Table S1 we report the combinations of the grooves' width (w) and grooves' gap spacing (g) used in the experiments to compare the fluidization with narrow and wide gaps (see also Fig. 1(a,b) in the manuscript for better visualization of the roughness geometry). We observed that random fluctuations of the channel height $H = 220\,\mu$m due to fabrication imperfections are below 5% as resulting from the analysis performed using a motorized optical microscope working with a depth of focus of $0.8\,\mu m$ at steps of $0.1\,\mu m$. Conversely, the patterning structures g, w and h have a reproducibility within 1%, the size being estimated by means of optical profilometer (SENSOFAR S neox, Spain) with a resolution of $0.2\,\mu$m. Using asymmetric channel configuration allows us to comapre slip velocities and plastic activity on smooth and rough walls in the same channel, further studies with symmetrical channels could provide better control over the wall stress.

TABLE S1. Summary of surface roughness patterns used in our experiments. Wide ranges of groove spacing (g) and post heights (w) were used.

g (μm)	w (μm)				
6*	6	8	-	20	-
8	-	8	15	-	37.5
15	-	8	15	-	37.5
20	-	8	-	20	-
37.5	-	8	15	-	37.5

*For technical reasons, in channels with gap spacing $g = 6\,\mu$m only the emulsions with $\Phi = 0.875$ was tested.

B. Bulk Rheology

The bulk rheology of the emulsion was measured using a stress controlled rotational rheometer (ARES 4400, TA Instruments, USA) with a cone-plate geometry (25 mm diameter, 0.04 radians). The flow curves follow the Herschel-Bulkley law, with parameters summarized in Table S2.

* ladislav.derzsi@unipd.it; Present address: Institute of Physical Chemistry of the Polish Academy of Sciences, Kasprzaka 44/52, 01-224 Warsaw, Poland

† sbragaglia@roma2.infn.it

‡ matteo.pierno@unipd.it

TABLE S2. Parameters for the bulk rheological flow curves according to the Herschel-Bulkley model $\sigma = \sigma_{\mathrm{Y}} + A\,\dot{\gamma}^n$, for various volume fractions Φ of the emulsions.

Φ	σ_0 (Pa)	A (Pa s$^{1/2}$)	n
0.8	22.16	19.91	0.5
0.85	40.99	27.82	0.5
0.875	55.14	31.41	0.5

C. Difference of the wall slip velocities normalized by the maximum (plug) velocity

In our experiments, for any fixed valur of g (also fixed pressure Δp and fixed volume fraction ϕ) varying only w (and thus λ) we have observed λ^{-1} scaling with only minor deviations (exponents estimates usually between -0.9 and -1.1, with very few exceptions). From the large set of experiments (using various pressures, w-g pairs and volume fractions) we got a large number of almost parallel λ^{-1} fitting lines. By normalizing them via the characteristic velocity in the center of the channel ($\mathrm{v}_{\mathrm{plug}}$) one can expect them to collapse into a single (in the recent paper into two) master curve. Deviations from an ideal collapse (data points seem somehow scattered) are due to fabrication imperfections of the microfluidic channels: there are slight differences in channel heights, some inlets are more clogged by the glue, etc. These differences may lead to fluctuations in the resistance of the channels, thus to variations of the flow velocity ($\mathrm{v}_{\mathrm{plug}}$) for a fixed pressure drop.

II. NUMERICAL SIMULATIONS AND PLASTIC REARRANGEMENTS DETECTION

The numerical simulations are based on a lattice Boltzmann model for emulsion droplets above the jamming point. Details on the numerical methodology can be found in [2–10]. The numerical setup of the Couette flow is the same as in [1]. To measure the displacement fields (see Fig. 4 in the manuscript) we consider Delaunay triangulations [11–13] built starting from the centers of mass of the emulsion droplets, and follow their evolution in time. Delaunay triangulation have already been used [1] to detect plastic rearrangements for wide gaps. In Figs. S1(a,b), we complement the results of [1] by comparing the distributions of plastic rearrangements for wide and narrow gaps. A plastic rearrangement takes place every time a link of the triangulation between two droplets disappears for boundary events (dashed segments between round points in Fig. S1(a)) and/or a new one appears (dashed segments between square points in Fig. S1(b)) for bulk events. Then, one can divide the domain in subregions with characteristic size equal to the mean droplet diameter d and count the total number of plastic rearrangements $N_{\text{plastic}}(\vec{x})$ in such a localized region. The local rate $\Gamma(\vec{x})$ follows

$$\Gamma(\vec{x}) = \frac{dN_{\text{plastic}}(\vec{x})}{dt}. \tag{1}$$

In Fig. S1(c) we report the spatial distribution of the rate of plastic rearrangements $\Gamma(\vec{x})$ for three different cases featuring the different gap g and width w at increasing λ. A reference case with a smooth wall is also displayed.

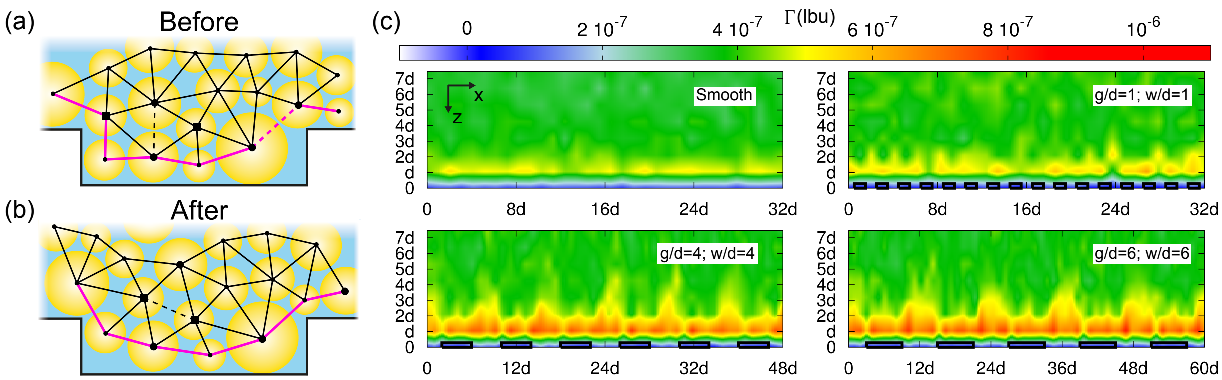

FIG. S1. (Color online). Panels (a) and (b) sketch two consecutive droplets configurations *before* (a) and *after* (b) the occurrence of events signaled by an edge-flip in the Delaunay triangulation of the centers of mass [12]. Round points in (a) connected by dashed lines get disconnected in (b) while disconnected square points in (a) get connected in (b) (only in the bulk). Purple segments highlight the boundary of the triangulation. In panel (c) the plastic activity rate $\Gamma(\vec{x})$ is reported in a color two-dimensional map for different roughness configurations. Results are reported in lattice Boltzmann units (lbu). Data for the smooth channel and $g/d = 6\,; w/d = 6$ are reproduced from [1].

[1] L. Derzsi, D. Filippi, G. Mistura, M. Pierno, M. Lulli, M. Sbragaglia, M. Bernaschi and P. Garstecki, *Phys. Rev. E*, 2017, **95**, 052602.
[2] R. Benzi, M. Sbragaglia, S. Succi, M. Bernaschi and S. Chibbaro, *J. Chem. Phys.*, 2009, **131**,.
[3] R. Benzi, M. Bernaschi, M. Sbragaglia and S. Succi, *Europhys. Lett.*, 2010, **91**, 14003.
[4] M. Sbragaglia, R. Benzi, M. Bernaschi and S. Succi, *Soft Matter*, 2012, **8**, 10773–10782.
[5] R. Benzi, M. Bernaschi, M. Sbragaglia and S. Succi, *Europhys. Lett.*, 2013, **104**, 48006.
[6] R. Benzi, M. Sbragaglia, P. Perlekar, M. Bernaschi, S. Succi and F. Toschi, *Soft Matter*, 2014, **10**, 4615–4624.
[7] R. Benzi, M. Sbragaglia, A. Scagliarini, P. Perlekar, M. Bernaschi, S. Succi and F. Toschi, *Soft Matter*, 2015, **11**, 1271–1280.
[8] B. Dollet, A. Scagliarini and M. Sbragaglia, *J. Fluid Mech.*, 2015, **766**, 556–589.
[9] A. Scagliarini, M. Sbragaglia and M. Bernaschi, *J. Stat. Phys.*, 2015, **161**, 1482–1495.
[10] A. Scagliarini, M. Lulli, M. Sbragaglia and M. Bernaschi, *Europhys. Lett.*, 2016, **114**, 64003.
[11] B. Delaunay, *Bulletin de l'Academie des Sciences de l'URSS,Classe des sciences mathematiques et naturelles*, 1934, **6**, 443–514.
[12] M. Bernaschi, M. Lulli and M. Sbragaglia, *Comput. Phys. Commun.*, 2017, **213**, 19 – 28.
[13] V. Mansard, A. Colin, P. Chaudhuri and L. Bocquet, *Soft Matter*, 2013, **9**, 7489–7500.